REAL-TIME INTERFEROMETRIC MONITORING SYSTEM FOR EXPOSURE CONTROLLED PROJECTION LITHOGRAPHY

Amit S. Jariwala[1,2], Robert E. Schwerzel[2], David W. Rosen[1]*

1 – George W. Woodruff School of Mechanical Engineering
Georgia Institute of Technology, Atlanta, Georgia, 30332
2 – AlpZhi ,Inc.
541 Tenth Street NW, Suite 121, Atlanta, Georgia, 30318
*Corresponding author. Tel.: +1 404 894 9668 Email: david.rosen@me.gatech.edu

Abstract:

Stereolithography is an additive manufacturing process in which liquid photopolymer resin is cross-linked and converted to solid polymer with an ultraviolet light source. Exposure Controlled Projection Lithography (ECPL) is a stereolithographic process in which incident radiation, patterned by a dynamic mask, passes through a transparent substrate to cure a photopolymer layer that grows progressively from the substrate surface. In contrast to existing stereolithography techniques, this technique uses a gray-scale projected image, or alternatively a series of binary bit-map images, to produce a three-dimensional polymer object with the desired shape, and it can be used on either flat or curved substrates.

Like most stereolithographic technologies, ECPL works in a unidirectional fashion. Calibration constants derived experimentally are fed to the software used to control the system. This unidirectional fabrication method does not, by itself, allow the system to compensate for minor variations, thereby limiting the overall accuracy of the process. We present here a simple, real-time monitoring system based on interferometry, which can be used to provide feedback control to the ECPL process, thus making it more robust and increasing system accuracy. The results obtained from this monitoring system provide a means to better visualize and understand the various phenomena occurring during the photopolymerization of transparent photopolymers.

1. Introduction

Exposure Controlled Projection Lithography (ECPL) is an additive manufacturing process used to build physical components out of a photopolymer resin. In conventional Stereolithography ("SLA"), a solid object is built layer by layer by exposing successive thin layers of photopolymer resin to a scanned laser beam. Recently researchers including Bertsch et al. [1], Chatwin [2], Monneret et al. [3], Sun et al. [4] and Limaye and Rosen [5] have demonstrated the use of a dynamic mask such as Texas Instruments' Digital Micromirror Device (DMD™) in conventional SLA instead of using a scanned laser beam. Some commercially available machines, such as the Perfactory® range of machines from EnvisonTec, Germany, also use one or more DMD™ chips to pattern the light in a conventional layer-by-layer SLA process [6]. Unlike these processes, ECPL utilizes the dynamic mask such that the irradiation from the DMD™ chip passes through a transparent substrate into a resin vat, and it uses careful control of the light intensity profile to define the vertical shape of the object being fabricated instead of the layer-by-layer approach used in conventional SLA processes. By using a gray-scale image, or alternatively a series of binary bitmap images, both the shape and the intensity profile of the irradiation can be controlled simultaneously; this in turn provides control over the photochemical

polymerization reaction in three dimensions. Similar techniques have been investigated by other researchers, in various forms. Erdmann et al. [7] have used mask projection stereolithography through transparent substrates for the fabrication of simple micro-lens arrays, and Mizukami et al. [8] have proposed the use of laser beam scanning through transparent substrates to cure photopolymers for the manufacture of micro-electrophoretic chips. However, to date there is a substantial lack of knowledge with regard to controlling the process in order to achieve the desired accuracy and precision over the final cured parts.

Limaye and Rosen [5] recently proposed a process planning method to control the lateral dimensions of the cured part in a conventional mask-based stereolithography process (then referred to as Mask Projection micro-SLA, or MPμSLA), although the proposed process plan was not intended to precisely control the curing front in the vertical dimension. Jariwala et al. [9] later proposed an elementary process planning method for controlling the cured profile of a thin film cured on a transparent substrate. The process planning method incorporated both a ray tracing model and a basic photopolymerization kinetic model to estimate the required fabrication parameters. Since the process plan was based on a simple polymerization model, the results showed deviations of up to 10% in all dimensions. It was hypothesized that the inaccuracies were largely the result of oxygen diffusion and inhibition during the polymerization process. Jariwala et al. [10] subsequently developed a photopolymerization model based on differential equations to model and simulate the effects of oxygen inhibition during polymerization. Although modeling the oxygen inhibition process provided results that more closely matched the observed experimental trends, the model was found inadequate to completely predict the exact shape of the cured part. Despite strong modeling efforts, it was found necessary to further investigate the photopolymerization process at the micron scale using real-time monitoring tools.

In this paper, a simple real-time monitoring system based on Mach-Zehnder interferometry is presented that enables us to monitor the growth of curing in the ECPL process. This monitoring system helps to better visualize and confirm the known photopolymerization phenomena, and it provides the basis for future real-time feedback control systems currently under development.

2. ECPL System

The block diagram of the ECPL process is illustrated in Figure 1. A UV light source is used with a 365nm filter and the light is passed onto the beam conditioning system. The objective of this beam conditioning system is to homogenize the light output from the light source and project it onto the Digital Micromirror Device (DMD™), which is used as a dynamic mask to project grayscale images. The projection system reduces the size of the image projected on the DMD™ and focuses in into the resin chamber. The resin chamber consists of a standard glass microscope slide which acts as a base, an identical glass slide which serves as a top, and spacers of various thicknesses depending on the dimensions of the object to be formed; the liquid photopolymer is placed inside this chamber.

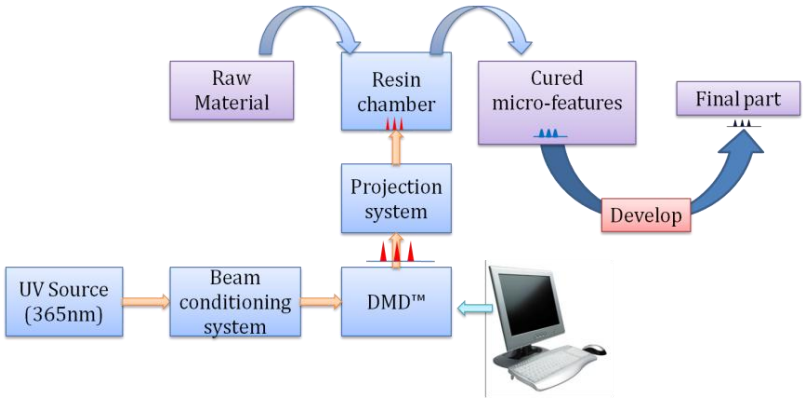

Fig. 1 Block diagram of the ECPL process

Grayscale images are formed on the DMD™ using the computer and projected from the DMD™ into the resin chamber. The regions of the liquid photopolymer resin which receive the irradiation cross-link and are converted into solid polymer, with a vertical profile that roughly matches the intensity profile of the incident light. The uncured monomer is then washed off the cured part in the "developing" process, and the final cured part is obtained on the glass slide. The following sections explain each of these modules in greater detail. Figure 2 shows photograph of the ECPL system installed at Georgia Tech.

UV light source: The light source used in our study was a commercial high-power mercury arc lamp with integral feedback control over the total irradiation intensity. Specifically, we used the Omnicure® S2000 UV spot curing system from Lumen Dynamics, which consists of a High Pressure 200 Watt Mercury Vapor Short Arc. The light from the lamp was delivered to the beam conditioning system using a 5mm light guide. The light spectrum resulting from this source is in the range of 320-500nm.

Beam conditioning module: The primary function of the beam conditioning module is to homogenize the light beam resulting from the light source and project it on the DMD™ chip. This module consists of a 365nm filter, a collimating lens, ground glass diffuser (from ThorLabs) and a UV coated mirror. The UV coated mirror is mounted on a kinematic mount which directs the light beam on the dynamic mask.

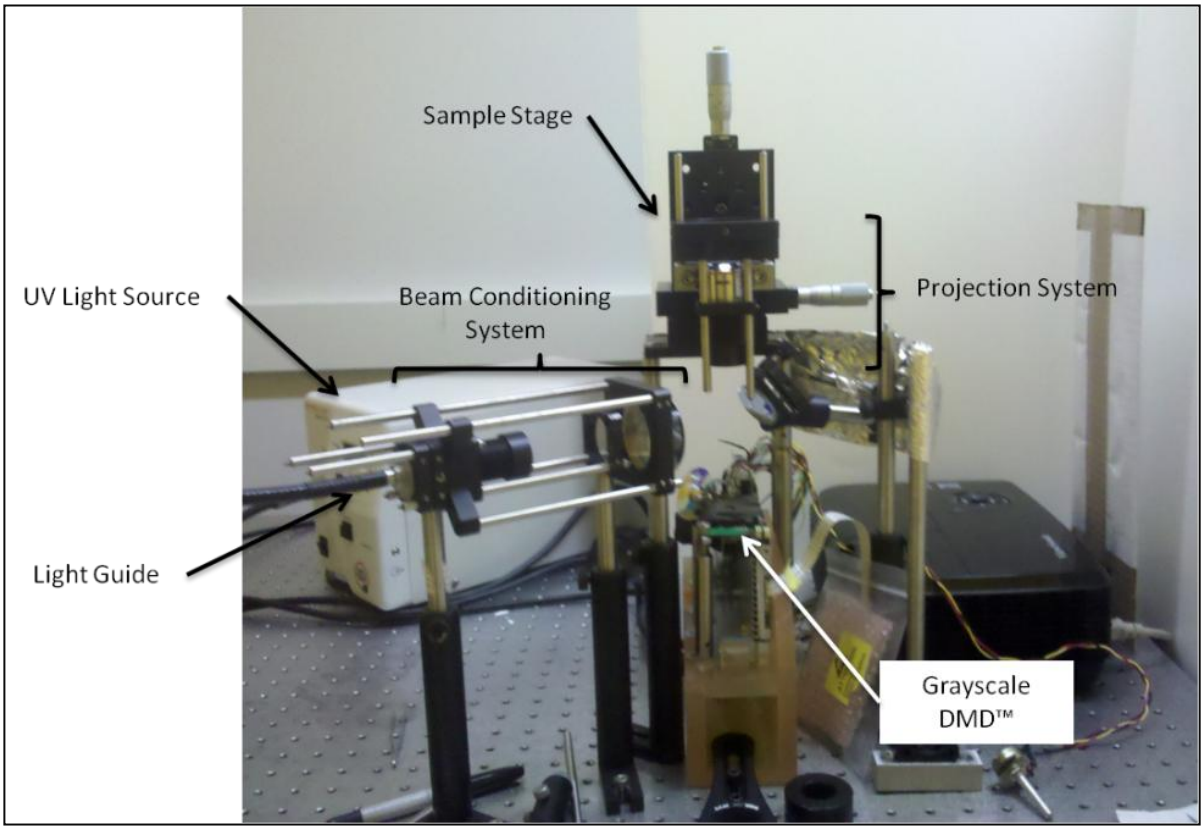

Fig. 2 Photograph of the ECPL system installed in Georgia Tech

DMD™: The Digital Micromirror Device (DMD™) is a product of Texas Instruments and is an array of individually addressable, bistable micro mirrors which can be selectively oriented to display any bitmap. Every pixel on the bitmap controls one and only one micromirror on the DMD™. The micromirrors are 12.65 µm square and the spacing between adjacent micromirrors is 1µm. The micromirrors in their neutral state are parallel to the DMD™ chip.

In its "ON" state, a micromirror swivels about its diagonal by 12° in one direction and in the "OFF" state, swivels by the same amount in the opposite direction. The DMD™ chip used in this study was obtained from a ViewSonic PJD 6221 projector. The bitmap displayed on the DMD™ serves as the object for the projection system, which is imaged on the resin chamber. PowerPoint software from Microsoft was used to create the images on the DMD™. The system is so designed such that a white image on the DMD™ reflects the light away from the projection system, resulting into no curing. Similarly, a black image results in projecting the image into the projection system, thus resulting into curing.

Projection System: The primary function of this system is to enlarge or reduce the image presented on the DMD™ and project it on the resin chamber. For this study, we used an infinite conjugate 4x UV microscope objective from Olympus. This objective was placed 160mm from the DMD™ window.

Resin Chamber: The resin chamber consisted of two glass slide stuck closely together with a spacer of known thickness placed along two edges as shown schematically in Figure 3. The resin is loaded between this sandwich structure of glass slides and is held by capillary force. The base glass slide acts as the substrate upon which the film is cured.

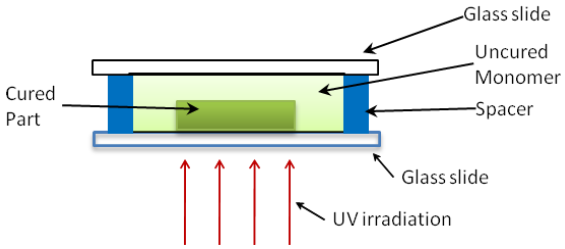

Fig. 3 Schematic of the resin chamber

3. Interferometric Cure Monitoring System

The basic principle of the interferometric monitoring system used in this study is based on the Mach-Zehnder interferometer. A coherent laser beam from a low-power red diode laser (670 nm wavelength) is directed at right angles into the photopolymer resin having a physical thickness **t** that is transparent at the wavelength of the laser. Interference occurs between the light reflecting from the front surface of the sample chamber (**a**) and the light reflecting from the back surface of the chamber (**b**) as shown schematically in Figure 4. Depending on the details of the experiment – the wavelength of the laser, the thickness of the material, the refractive index of the material at the wavelength of the laser – the interference can be either constructive, leading to an increase in the intensity of the reflected beam, or destructive, leading to a decrease in the intensity of the reflected beam. The result is that if the material being examined is reactive upon UV irradiation, as our photocurable resins are, the refractive index of the material will typically increase as density of the resin increases as it polymerizes;

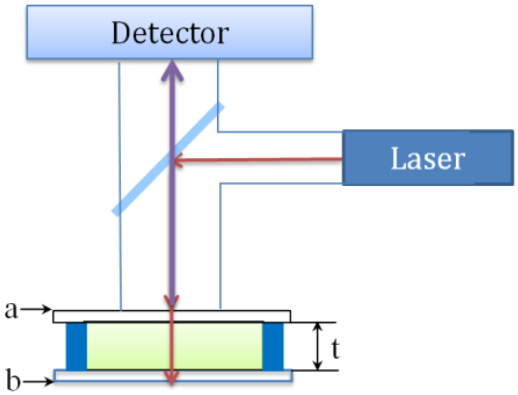

Fig. 4 Schematic of the cure monitoring system

the intensity of the reflected laser beam will therefore exhibit a periodic modulation of maxima and minima as the front-surface and back-surface reflections go in and out of phase with one another.

Other researchers have also employed interferometry to monitor photopolymerization reactions, using either Michelson [11, 12] or Mach-Zehnder [13, 14] interferometer configurations. However, these prior schemes have all used elaborate, delicate optical systems with multiple mirrors and beam-splitters, making them expensive and time-consuming to set up. In contrast, by using the reflections from the front and back surfaces of the sample chamber itself as the basis of our interferometer, we have been able to obtain comparable results with excellent signal-to-noise ratios in a simple, robust experimental configuration. While our current system is a single-beam apparatus in which the laser beam interrogates only the region of the sample undergoing photopolymerization, it would be a simple extension of the system to incorporate a second, reference beam that would monitor a spot on the sample away from the irradiation zone. The output from this reference interferometer could then be electronically subtracted from the output of the photopolymerization interferometer to give a compensated signal that automatically zeroed out any variations resulting from temperature changes, shrinkage or expansion of the photopolymer, and so on. Alternatively, if desired, the output from the reference interferometer could be monitored directly to provide a measure of, for example, whether shrinkage was changing the physical path length ***t*** to a significant extent.

We have successfully demonstrated the feasibility of using our system to monitor the photopolymerization process in real-time by adapting our ECPL apparatus to incorporate a glass microscope slide inclined at 45 degrees to serve as a beam splitter to direct the laser beam into the sample chamber, and a custom-made detector module incorporating a Texas Instruments OPT-101P photodetector chip, as shown in Figure 5. This chip includes built-in circuitry that enables it to provide a linear voltage output in response to changes in the detected light intensity, making it ideal for our purposes. The output was coupled to a lab computer via a National Instruments A-to-D module. We note that the the beam splitter and the normal incidence geometry that we have employed was adopted solely for conveniently adapting our current ECPL apparatus to accommodate the interferometric cure monitor; the experimental results, and the analysis principles described below, would be the same if the laser and detector were mounted symmetrically off-axis to each other with no mirrors or beam-splitters, provided only that the angle of incidence (measured from the normal) for both the laser and the detector was small, typically less than 10° or so.

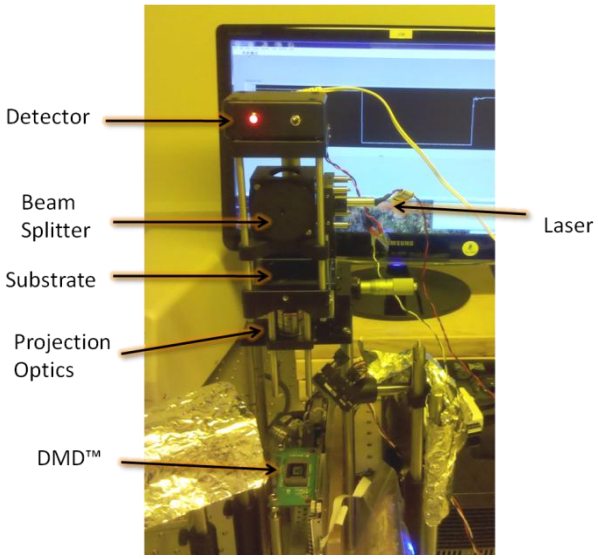

Figure 5. Photograph showing part of the ECPL system (full picture in Figure 2) with the components of the interferometric monitoring system

4. Working Principle

The real-time monitoring system is based on the principle of interferometry, which is capable of detecting changes in the refractive index of the sample during the course of the photopolymerization reaction. Referring to Figure 4, the monitoring system detects the difference in the optical path lengths between the light reflected from the top air-glass interface (marked by 'a') and the bottom glass-air interface (marked by 'b'). This is so because of the maximum difference in refractive index between these two interfaces of glass and air. The refractive index of air is 1, that of the glass slide is 1.55 and that of the resin is 1.4723 [15], and the greatest reflections occur from the surfaces where the difference in refractive index is greatest. In our configuration, the upper and lower surfaces of the glass sample chamber form the basis of a Mach-Zehnder interferometer, without the need for any additional mirrors or optical complexity.

The optical path length of light in any medium is given by:

$$L = nl = nt/\cos\theta \quad (1)$$

where L is the optical path length, n is the refractive index of the medium through which the light travels, l is the physical path length of the light in the medium, t is the physical thickness of the medium, and θ is the angle of incidence of the light, as measured from the normal to the plane of the sample. From figure 4, the total round optical path length resulting from traveling through the top glass slide, reflecting from the bottom glass slide, and traveling back to the top of the top glass slide can be calculated as:

$$L_t = (4\, n_g t_g + 2\, n_s t_s)/\cos\theta \quad (2)$$

where L_t is the total optical path length for light travelling though the sample and back. n_g & n_s are the refractive indices of glass slide and the sample and t_g & t_s are the thickness of the glass slides (assuming that thickness of both the top and bottom glass slides are same, which is indeed the case for our experiments) and thickness of the spacer, which is the same as the thickness of the photopolymer resin in the sample cell). If the refractive index of the sample material changes during the measurement, as is expected for a photoreactive material being irradiated, the resulting change in the optical thickness of the material is then given by:

$$\Delta L_t = 2\, \Delta n_s t_s/\cos\theta \quad (3)$$

Since the refractive index of the glass slides does not change, this does not contribute to the change in interference condition during the reaction. Moreover, for small angles of incidence (typically less than around 10°, where the value of cos θ is very close to 1.00), Equation 3 can be simplified to a good approximation as simply:

$$\Delta L_t = 2\, \Delta n_s t_s \quad (4)$$

This can be expressed as a fraction of the laser wavelength, or the Wave Shift, by

$$\text{Wave Shift} = \Delta L_t / \lambda \quad (5)$$

For our purposes, the direction of the intensity change (increase versus decrease) is unimportant, since each measurement starts at a completely arbitrary reflected intensity and we have no control over the initial interference condition of the front-surface and back-surface reflected laser beams. However, as will be seen below, changes in the direction of the intensity change (that is, phase reversals) that occur during a measurement are nonetheless quite

informative, as they can signal a change in process from photochemical cure (typically resulting in shrinkage) to thermal expansion due to warming of the material, or from warming of the sample material during the irradiation to cooling back to room temperature after the irradiation.

The overall intensity of the reflected laser beam follows a cosine curve as a function of the Wave Shift, with a maximum intensity when the wave crests of the electric field vectors of the front-surface reflection match up with the wave crests of the electric field vectors of the back-surface reflection, and minimum intensity when the two sets of wave crests are exactly out of phase with one another. It is therefore more useful to express the Wave Shift of Equation 5 as a Phase Shift, Ø, with units of 2π radians of phase difference between the wave crests of the two beams.

$$Ø \text{ (radians)} = 2 \pi \Delta L_t / \lambda = 2 \pi (2\Delta n_s t_s) / \lambda = 4 \pi \Delta n_s t_s / \lambda \quad (6)$$

In general, for any arbitrary phase shift Ø (not necessarily a maximum or a minimum of the reflected laser beam intensity), the refractive index change responsible for the phase shift will be given by:

$$\Delta n_s = \lambda Ø / 4 \pi t_s \quad (7)$$

and for the specific case where λ = 670 nm = 0.670 microns (for a typical red diode laser),

$$\Delta n_s = 0.053 Ø / t_s \quad (8)$$

where Ø is expressed as the measured total number of π radians of phase shift and t_s is the physical thickness of the photopolymer sample in microns.

Alternatively, the same relationship can be expressed as:

$$Ø = 18.87 \Delta n_s t_s \quad (9)$$

We thus find a linear relationship between the total phase shift and the change in the refractive index that occurs during the reaction. Because the photopolymer curing reaction propagates vertically through the resin sample as the irradiation proceeds, the change in refractive index is tied directly to the height of the cured polymer within the resin sample. Thus, the observed phase shift is also a direct measure of the height of the cured region of polymer as the reaction proceeds. We note that this analysis assumes that the physical thickness of the sample chamber does not change during the irradiation, which is appropriate in our case given the rigidity of the glass slides used to form the sample chamber and the small area (typically less than 1 mm^2) of the photopolymer that is irradiated in any given experiment.

5. Experimental Procedure

The resin in the reaction chamber was cured by the UV irradiation patterned by the bitmaps on the DMD™. Because our DMD™ chip was capable of projecting gray-scale images, we typically used only a single gray-scale image which included both the shape of the object we wished to fabricate and a gray-scale gradient that was developed to compensate for any residual irradiation inhomogeneity. We used a tri-functional acrylate monomer - trimethylolpropane triacrylate (TMPTA, SR-351) obtained from Sartomer and used as obtained, with 5% by weight of the photoinitiator 2, 2-dimethoxy-1, 2-diphenylethan-1-one (DMPA, IRGACURE-651) obtained from Ciba Specialty Chemicals, as the resin composition. This composition allows for 92% transmission of visible spectrum when completely cured. The exposure intensity was

controlled by directly setting the intensity levels on the light source. The exposure time was controlled by setting the time of projecting a slide on the projector through the options provided by the PowerPoint software by Microsoft. We used an aqueous surfactant based solution to wash the samples, followed by blowing the uncured resin with nitrogen gas. The height of the cured parts was measured by a 3-D non-contact confocal microscope.

6. Typical Interferogram

A representative example of the data provided from the interferometric cure monitoring system is shown below in Figure 6 for a 250-micron thick sample. A number of salient features are evident from the figure. An initiation period is clearly visible at the left side of the trace as dissolved oxygen and inhibitors in the photoinitiator are scavenged before the polymerization process can get underway. Then, toward the right side of the trace, a continuing densification that we ascribe to dark reaction is apparent after the irradiation has stopped, followed by eventual equilibration. About 27.5 full oscillations of the intensity are visible, corresponding to a total phase shift of approximately 173 radians. These oscillations are a result of the changes in refractive index and the height of the part cured. By monitoring the number of oscillations during the curing process, we can estimate the height of the cured part, and this estimate can be calibrated by subsequent measurement of the height of the cured part as described above.

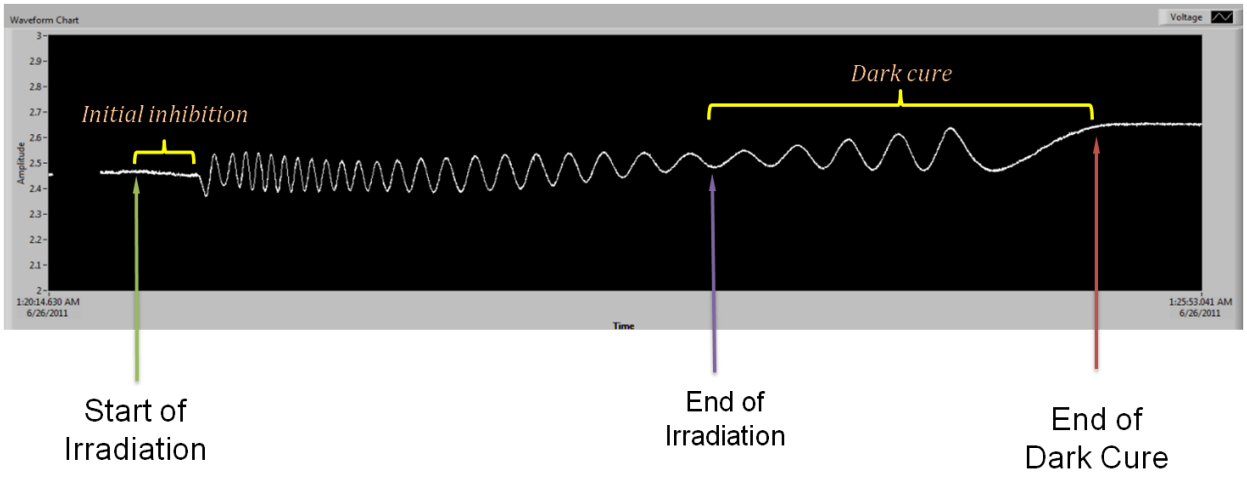

Figure 6. Results from interferometric monitoring system for curing a 250 micron thick sample. Horizontal X-axis corresponds to time and the Y-axis shows the output voltage detected from the photodetector

7. Results and Discussion

The real-time interferometric cure monitoring system was used to visualize the photopolymerization reaction and study the polymerization phenomena in more detail.

To confirm the reproducibility of the interferometric measurements, three samples were cured with the same exposure dose and intensity. The results from the three experiments are shown in three different colors in Figure 7a. It is to be noted that the charts are plotted on arbitrary intensity units and only the number of oscillations in the signal are of importance (the three curves differ somewhat in shape because the initial phase relationship between the front

and back reflections differs slightly from sample to sample). The key result is that all the three samples yielded essentially the same number of oscillations, and therefore the same total phase shift and the same overall change in refractive index, over the course of the reaction. The final height of each cured part was measured to be around 122µm.

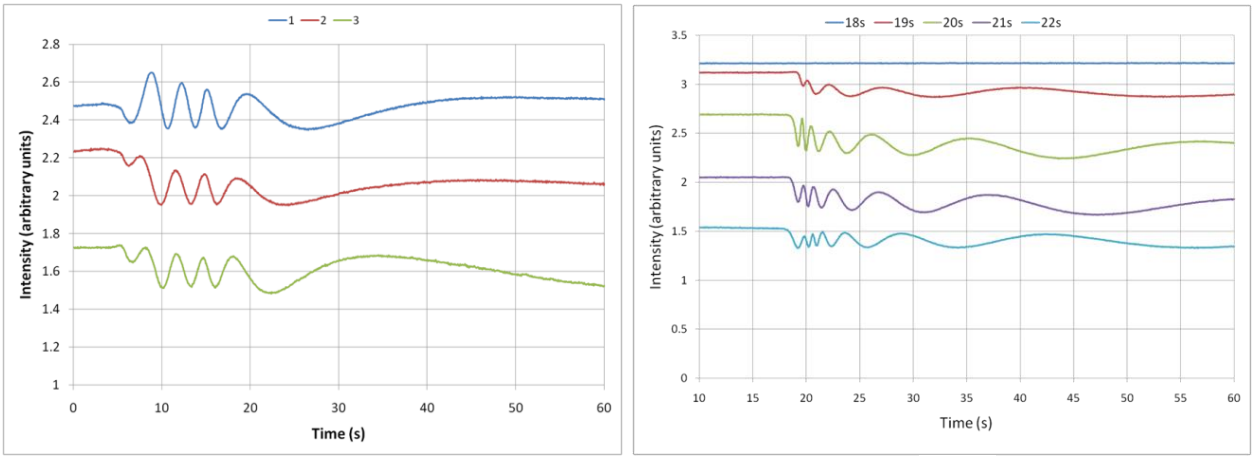

a) b)

Fig. 7 Results from the Interferometric Cure Monitoring System.
a) Results from three consecutive experiments showing consistent results
b) Results showing effect of varying total exposure dose (exposure time varied)

The interferometric monitoring system also helps in visualizing the growth of polymerization. An interesting result of these experiments is that the photoinitation period of ~19 seconds remains more or less constant under our conditions over the various experiments conducted with the same batch of resin. The number of fringes also increases with increasing total exposure dose, as would be expected from the increased total densification as the cured part height increases; this effect is shown n Figure 7b.

One of the primary objectives for incorporating this live monitoring system was to assist in estimation of the height of the cured part in real time. Figure 8 shows the preliminary correlation that was observed between the measured height of the cured part after washing and flood cure (by confocal microscopy) and the corresponding total phase angle. Blue dots represent actual experimental data points. It should be noted that the final cured part was washed in an aqueous solution followed by blowing with nitrogen gas and post curing by flood exposure with 365nm light prior to measuring its height; we ascribe the slight deviations from linearity in Figure 8 to distortions in the shape of the cured part introduced by the washing procedure prior to flood cure.

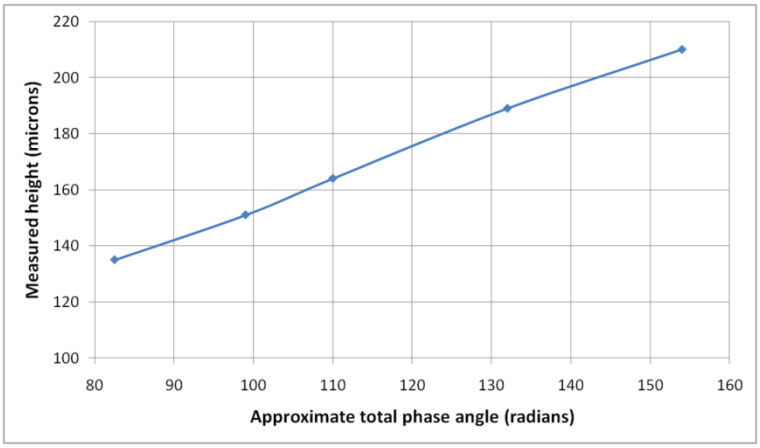

Fig. 8 Results showing the height correlation with total phase angle

In order to further explore the utility of the monitoring system, we conducted experiments to highlight the effects of chemical inhibition (caused by dissolved oxygen and inhibitors) on photopolymerization. Specifically, we conducted experiments by varying the spacer thickness, thus varying the thickness of the sample chamber, ***t,*** as shown in Figure 9a. The two plots were obtained from two different experiments, where the samples were irradiated at the same intensity for 25 seconds. No curing was observed when using a thicker spacer (1.4mm), whereas a different sample of the same resin was cured easily to a height of 106µm when using the thinner, 200µm spacer. This phenomenon was never considered when using the conventionally accepted one-dimensional Beer Lambert's law for photopolymerization. We ascribe this effect to continued inhibition of the photopolymerization reaction by rapid diffusion of dissolved oxygen into the irradiation zone from the larger reservoir of air-saturated resin in the thicker sample.

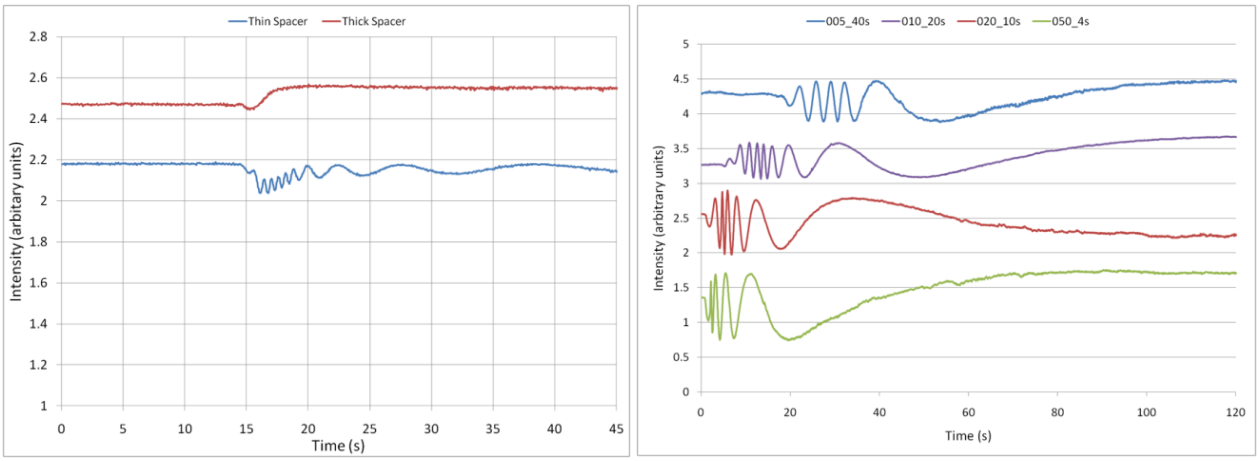

a) b)

Fig. 9 Results from the Interferometric Cure Monitoring System.
a) Results by varying the sample cell thickness
b) Results showing effect of varying exposure intensity (total exposure dose kept constant)

Another interesting result obtained from the live monitoring system was the effect of irradiation intensity on the course of the photopolymerization reaction, as shown in Figure 9b. Four experiments were conducted by providing the same total energy dose (800µJ/cm^2) but varying the intensity from 20µW/cm^2 (40s exposure) to 200µW/cm^2 (4s exposure). It was observed that the initial photoinitiation period is progressively reduced with higher exposure intensities, as expected from the reaction kinetics; with greater light intensities, the rate of free radical formation from the photoinitiator is greater, so dissolved oxygen and other inhibitors are scavenged more rapidly and the photopolymerization reaction can then proceed more quickly. Our interferometric cure monitor provides a direct window into the details of this process, in real time.

8. Conclusions

This paper presented an approach to monitor the growth of photopolymerized part in the ECPL process in real time. Our results show that the system can be used to estimate the height of the cured part in real time during the irradiation, that it can provide valuable insights into the effects of dissolved oxygen on the initiation and progression of the photopolymerization

reaction, and that it can monitor the progress of the dark polymerization reaction that continues for some time after the irradiation has been stopped as residual reactive "living polymer" radicals are gradually scavenged or otherwise terminated. The presented method could be further improved to provide real time feedback to the ECPL process thus improving the overall accuracy of the process.

9. Acknowledgements

This material is based upon work supported by the National Science Foundation under Grant No. IIP 1047095. The authors are also thankful to the support provided by the Georgia Research Alliance VentureLab grant for technology commercialization.

10. References

[1] Bertsch A., Zissi S., Jezequel J., Corbel S. and Andre J., 1997, "Microstereolithography Using Liquid Crystal Display as Dynamic Mask-Generator", *Microsystems Technologies,* **3**(2), pp. 42-47.

[2] Chatwin C., Farsari M., Huang S., Heywood M., Birch P., Young R., Richardson J., 1998, "UV Microstereolithography System That Uses Spatial Light Modulator Technology", *Applied Optics,* **37**(32), pp. 7514-22.

[3] Monneret S., Loubere V., Corbel S., 1999, "Microstereolithography Using Dynamic Mask Generator and A Non-Coherent Visible Light Source", *Proc. SPIE,* **3680**, pp. 553-561.

[4] Sun C., Fang N., Wu D.M., Zhang X., 2005, "Projection Micro-Stereolithography Using Digital Micro-Mirror Dynamic Mask", *Sensors and Actuators A,* **121**, pp. 113-120.

[5] Limaye A. and Rosen D., 2007, "Process Planning Method for Mask Projection Micro-Stereolithography", *Rapid Prototyping Journal,* **13(**2), pp. 76-84

[6] Referred website: http://www.envisiontec.de; visited on 15th July, 2011.

[7] Erdmann L., Deparnay A., Maschke G., Längle M., Bruner R., 2005, "MOEMS-Based Lithography for the Fabrication of Micro-Optical Components", *Journal of Microlithography, Microfabrication, Microsystems,* **4**(4), pp. 041601-1, -5.

[8] Mizukami Y., Rajnaik D., Rajnaik A., Nishimura M., 2002, "A Novel Microchip for Capillary Electrophoresis with Acrylic Microchannel Fabricated on Photosensor Array", *Sensors and Actuators B,* **81**, pp. 202-209.

[9] Jariwala A., Ding F., Zhao X., Rosen D., 2008, "A Film Fabrication Process on Transparent Substrate Using Mask Projection Stereolithography", D. Bourell, R. Crawford, C. Seepersad, J. Beaman, H. Marcus, eds., *Proceedings of the 19th Solid Freeform Fabrication Symposium*, Austin, Texas, pp. 216-229.

[10] Jariwala A., Ding F., Boddapati A., Breedveld V., Grover M. A., Henderson C. L., Rosen D. W., 2011, "Modeling effects of oxygen inhibition in mask-based Stereolithography", *Rapid Prototyping Journal*, **17**(3), pp. 168-175.

[11] O. Dudi and W. T. Grubbs, 1999, "Laser interferometric technique for measuring polymer cure kinetics", *Journal of Applied Polymer Science,* **74**, pp. 2133-2142.

[12] E. A. Fogleman, M. T. Kelly, and W. T. Grubbs, 2002, "Laser interferometric method for measuring linear polymerization shrinkage in light-cured dental restoratives", *Dental Materials*, **18**, pp. 324-330.

[13] K. Inoue, S. Komatsu, X-A Trinh, T. Norisuye, and Q. Tran-Cong-Miyata, 2005, "Local deformation in photo-crosslinked polymer blends monitored by Mach-Zehnder interferometry", *Journal of Polymer Science: Part B: Polymer Physics*, **43**, pp. 2898-2913.

[14] Q. Tran-Cong-Miyata, D.-T. Van-Phem, K. Noma, T. Norisuye, and H. Nakanishi, 2009, "The roles of reaction inhomogeneity in phase separation kinetics and morphology of reactive polymer blends", *Chinese Journal of Polymer Science*, **27**(1), pp. 23-36.

[15] http://www.sartomer.com/wpapers/20551.pdf; visited on 15th June, 2011.